J. Fluid Mech. (1997), *vol.* 350, *pp.* 295–310. Printed in the United Kingdom

On the shape of flames under strong acoustic forcing: a mean flow controlled by an oscillating flow

By D. DUROX[1], F. BAILLOT[2], G. SEARBY[3] AND L. BOYER[3]

[1]Laboratoire EM2C, CNRS/ECP, 92295 Châtenay-Malabry, France
[2]CORIA, CNRS/Université de Rouen, 76821 Mont Saint-Aignan, France
[3]IRPHE, CNRS/Université de Provence, 13397 Marseille Cedex 20, France

(Received 17 May 1996 and in revised form 23 June 1997)

A conical flame, in the presence of high-frequency (≈1000 Hz) and high-amplitude acoustic modulation of the cold gases, deforms to a shape which is approximately hemispherical. It is shown that the acoustic level required to produce a hemispherical flame is such that the ratio of acoustic velocity to laminar combustion velocity is about 3. This flame flattening is equivalent to the phenomenon of acoustic restabilization observed for cellular flames propagating in tubes. The transition between the conical flame and a hemispherical flame is described. The surface area of the reaction zone of the flame is found to be unmodified when the flame flattens. The velocity field at the burner outlet is examined with and without a flame. The mean flow lines are strongly deflected when the hemispherical flame is present. We show that the presence of the flame creates an unusual situation where the oscillating flow controls the geometry of the mean flow.

1. Introduction

Thermo–acoustic interactions can substantially modify flame behaviour. In confined situations, these interactions can lead to intense acoustic instabilities, sometimes sufficient to damage combustion chambers. In the literature there exists considerable work, using simple configurations, to elucidate the physical mechanisms involved in the interaction between flames and acoustic fields. The configurations investigated include flame propagation in tubes (Dunlap 1950; Markstein 1953, 1964; Kaskan 1953; Leyer & Manson 1971; Poinsot *et al.* 1987; Clavin, Pelcé & He 1990; Searby & Rochwerger 1991; Pelcé & Rochwerger 1992; Searby 1992; Clanet & Searby 1994) or flames anchored on grids inside tubes (Le Helley 1994).

Experiments on flames stabilized in an acoustic field above a burner are less numerous and more difficult to interpret, although this configuration is complementary to the case of flames in tubes. Baillot, Durox & Prud'homme (1992), Bourehla (1994), Durox, Schultz & Rudent (1995) have used a periodic modulation of the velocity field at the exit of a nozzle burner. They have observed the effect of the oscillating velocity field on the behaviour of flames and have analysed the sensitivity of flames to perturbations of small amplitude. They have noted that, for small values of velocity modulation ($< 15\%$), flames respond only at low frequency; for frequencies higher than 300 or 400 Hz, and for weak perturbations, flames are not deformed and conserve the conical form that they have when there is no excitation.

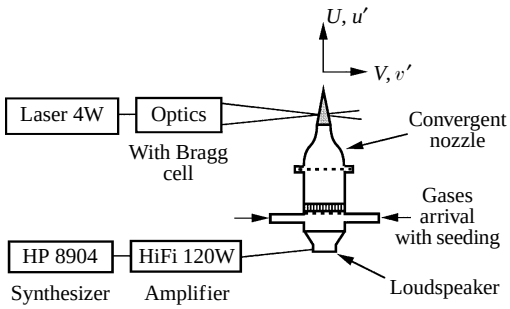

FIGURE 1. Experimental set-up.

In 1943, von Hahnemann & Ehret working with higher frequencies, around 1000 Hz, and with high acoustic amplitudes, observed a striking deformation of a conical flame, which adopted the form of a flattened hemisphere and appeared to be motionless above the burner. They compared the shape of the flame front obtained by strioscopy with the equipotential surfaces of an electrostatic analogy of the acoustic velocity field. They also concluded that there was a small decrease in the surface area of the flame, but the accuracy of their experimental technique was limited. De Sœte (1964) has also observed this flattening of a conical flame under strong acoustic excitation. He attributed the change of shape to a modification of the internal structure of the front.

This surprising effect of an acoustic field on the behaviour of a flame front has never been explained and the purpose of this paper is to provide new insight into the mechanism leading to such a strong modification of the flame shape and the associated flow field at the exit of the burner tube. To do this, we first repeat the experiment using modern investigation techniques. This paper deals with the motion of the front, the modification of the upstream velocity field and the transition between a conical and a hemispherical flame. A systematic comparison is made between the flow with a flame and the flow without a flame. The phenomenon is compared to the behaviour of flames propagating in tubes in the presence of an acoustic field.

2. The experimental apparatus

2.1. *The burner and the acoustic excitation*

Experiments were carried out with the configuration shown in figure 1. The burner consists of a convergent stainless-steel nozzle of 2.2 cm exit diameter, followed by a cylindrical end piece 2 cm long. The contraction ratio of the nozzle was 8.7. A cylindrical tube 15 cm long, containing various grids and honeycombs to produce a laminar flow at the exit, was placed upstream from the convergent nozzle. A loudspeaker, fed by a 120 W power amplifier, occupied the base of the burner. Sine wave excitation was provided by an HP 8904 synthesizer.

2.2. *Measurement techniques*

Gas velocities were measured by laser Doppler velocimetry (LDV). The system included a 4 W argon laser, an optical system with a Bragg cell and a photo-multiplier situated in forward scattering mode. The digital output of the LDV counter was processed on a micro-computer. The transverse velocity component was measured by rotating the optical system. This was not a problem since the flame could be

maintained perfectly stable for long periods. Oil droplets were used to seed the flow. The mean diameter of the droplets was less than 2 μm (Durox & Baillot 1993). Typical measurement rates were 4×10^3 s^{-1} and velocity statistics were collected over 8×10^3 samples. Visualizations were made by laser tomography (Boyer 1980) with the same laser and seeding. The flame was continuously recorded at 50 frames per second using a CCD video camera. The exposure time could be set between 1/60 and 10^{-4} s. The images were post-processed from the video tape.

All the experiments were carried out at atmospheric pressure with a methane–air mixture at a fixed equivalence ratio of 1.05. This equivalence ratio corresponds to the maximum propagation velocity of the premixed flame, $U_L = 0.4$ m s^{-1}. The latter is thus insensitive to any small variations of the mixture ratio. Moreover, lean flames are subject to blow-off whilst rich flames are surrounded by a diffusion flame which can introduce an additional complication. The gas flow rate was fixed at a value corresponding to a space-averaged flow velocity of 0.92 m s^{-1} ($\approx$ 1.3 m s^{-1} on the burner axis). The Reynolds number based on the burner diameter was thus 1450. The acoustic excitation was sinusoidal at a fixed frequency of 950.1 Hz. The images from the CCD camera thus showed an apparent (stroboscopic) frequency of 0.1 Hz. The signal amplitude from the generator was initially adjusted to obtain a stable hemispherical flame and was kept constant for all measurements presented here, with or without a flame. This acoustic level produced a modulation of the axial velocity of 150% (i.e. including flow reversal). The amplitude of excitation was changed only in the study of the transition between the conical flame and the rounded flame.

It was verified that the flow at the burner exit oscillated at 950.1 Hz and had no notable harmonic content in the spectrum of the axial velocity component. The velocity spectrum was measured on the axis of the burner at 1.5 mm above the exit. The flame surface area was measured using the downstream limit of the luminous zone of the flame, visible in figures 5, 7 and 8.

3. Comparison of the velocity fields with and without a flame

3.1. *Flow without flame*

In the absence of acoustic excitation, the cold flow at the burner exit (not shown) is a laminar plug flow with a quasi-top-hat profile which evolves little over several centimetres. Kelvin–Helmholtz vortices develop only further downstream, well beyond the position corresponding to the maximum extent of the flame.

In the presence of the acoustic excitation, the flow is modified. Two instantaneous views of the flow at the burner exit are shown in figure 2. The streamlines in the centre of the burner are vertical over a distance of about 1 cm. The exterior of the flow is laterally agitated and more or less regular structures appear, figure 2(*a*). Periodic radial ejections are observed, just above the exit plane of the burner, figure 2(*b*). They are generated by the pressure gradient; the acoustic pressure node is not situated in the exit plane of the tube but at a downstream distance roughly equal to the radius of the tube (Bruneau 1983). During part of the acoustic cycle, the pressure just above the exit plane is higher than the ambient pressure creating a radial flow. At other times, the jet contracts towards the centre and the zones close to the burner periphery are unseeded.

The profiles of the mean axial and radial velocities U, V and of the r.m.s. oscillating components u', v' along the downstream axis are shown in figure 3. Up to 20 mm downstream, the mean axial velocity, varies little and remains close to 1.2 m s^{-1},

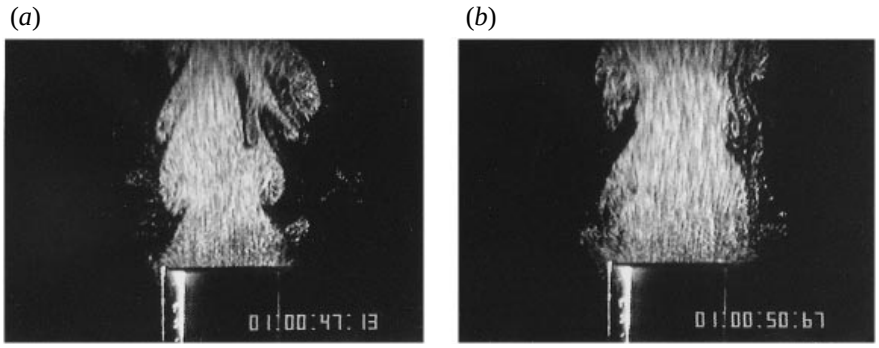

FIGURE 2. Two views of the inert flow. Exposure time: 1/500 s. Space-averaged flow velocity: 0.92 m s^{-1}. Frequency: 950.1 Hz.

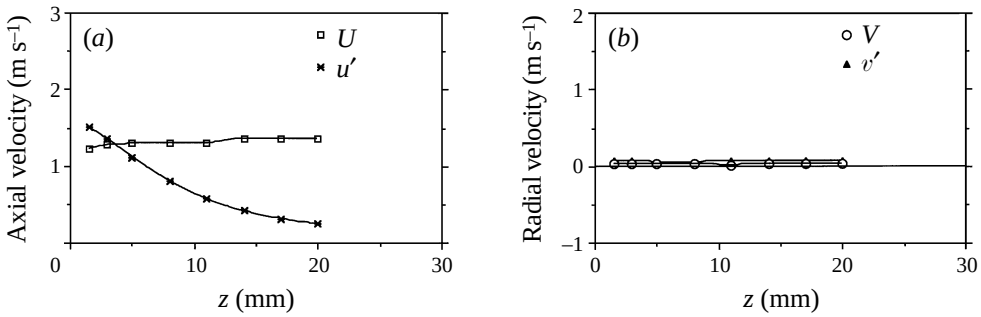

FIGURE 3. Streamwise profiles the velocities in the cold flow. U and V are the mean axial and radial velocities, u' and v' are the corresponding r.m.s. components of the oscillation. Space-averaged flow velocity: 0.92 m s^{-1}. Frequency: 950.1 Hz.

showing that the mixing with the ambient air and the resulting deceleration have not yet reached the centre of the flow. The slight increase in velocity with downstream distance in the presence of acoustic forcing is reproducible and outside statistical errors. We attribute this behaviour to a slight asymmetry between the inflow and outflow. It is known that boundary-layer flow separation can occur during high-amplitude outgoing acoustic flow from an open pipe, but there is no flow separation during the incoming half-cycle (Ingard & Ising 1967). The amplitude of the r.m.s. acoustic velocity, u', decreases regularly from 1.5 m s^{-1} at the exit of the burner down to 0.2 m s^{-1} at $z = 20$ mm. This is compatible with a divergent oscillating flow centred on the burner exit.

The instantaneous velocity at the burner exit thus oscillates between -0.92 m s^{-1} and $+3.32$ m s^{-1} and consequently there is a substantial reverse flow during each acoustic cycle. However the corresponding amplitude of displacement is small : 7.1×10^{-4} m. On the axis, the peak acceleration is 12 600 m s^{-2} (i.e. $\approx$ 1290 g). The radial velocities on the burner axis are negligibly small.

Two radial profiles of the axial velocity are presented in figure 4(*a*). At $z = 1.5$ mm above the exit, the mean axial velocity is almost constant between $y = -7$ mm and $+7$ mm but decreases rapidly at the edge of the burner. We observe an apparent negative mean velocity just outside the burner. This is a bias produced by the fact that the reverse flow pulls unseeded air into the measuring volume and thus, in this region, the mean velocity is not averaged over a complete acoustic cycle. The r.m.s.

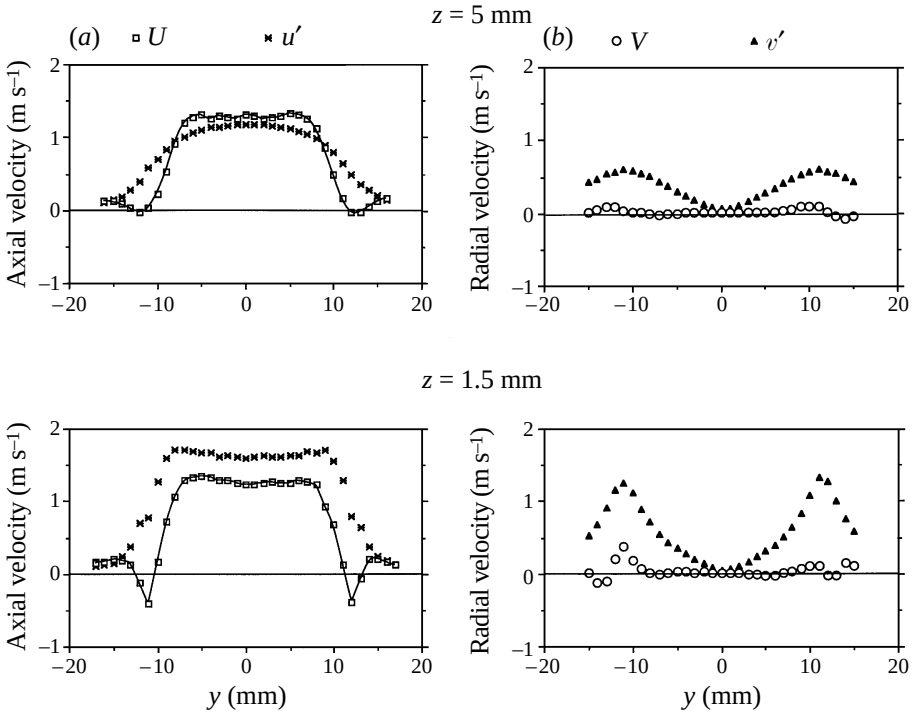

FIGURE 4. Radial velocity profiles measured at $z = 1.5$ mm and $z = 5$ mm above the burner in the cold flow. U and V are the mean axial and radial velocities, u' and v' are the corresponding r.m.s. components of the oscillation. Space-averaged flow velocity: 0.92 m s^{-1}. Frequency: 950.1 Hz.

velocity u' is also approximately constant in the same zone (-7 mm and $+7$ mm). At $z = 5$ mm, the profile of the mean velocity is slightly widened but the velocity remains constant between -6 mm and $+6$ mm. There are no negative velocities. The profile of u' is considerably widened and decreases progressively from the centre outwards.

Two profiles of the radial velocity, V, at $z = 1.5$ mm and at $z = 5$ mm are shown in figure 4(*b*). At these two distances downstream, the average radial velocity is close to zero indicating that the *mean* flow is almost vertical. However the oscillating radial component is strong near the boundary of the jet; the radial r.m.s. component v' reaches 1.3 m s^{-1} at $y = 11$ mm and $z = 1.5$ mm. Further downstream, at $z = 5$ mm, the modulation is smaller. It is important to note that the radial and axial velocity fluctuations are in phase at the acoustic frequency. This is apparent from the streamlines of figure 8.

In summary, the total flow in the cold jet can be interpreted as the superposition of a vertical mean flow and an oscillating flow which is the near-field flow of the sound radiation from the burner exit. At larger distances the burner can be regarded as a point source of acoustic waves.

3.2. *Flow with a flame*

3.2.1. *No acoustic excitation*

A tomographic cut through the laminar flame without acoustic excitation is shown in figure 5. The flame is almost conical and the particle trajectories are almost parallel to the axis except close to the burner edge where an outwards deflection is observed, due to the combined effects of the boundary layer and the resulting flame curvature.

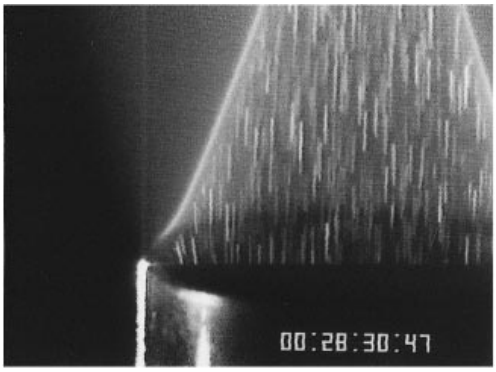

FIGURE 5. Tomographic cut through the laminar flame. Equivalence ratio: 1.05.

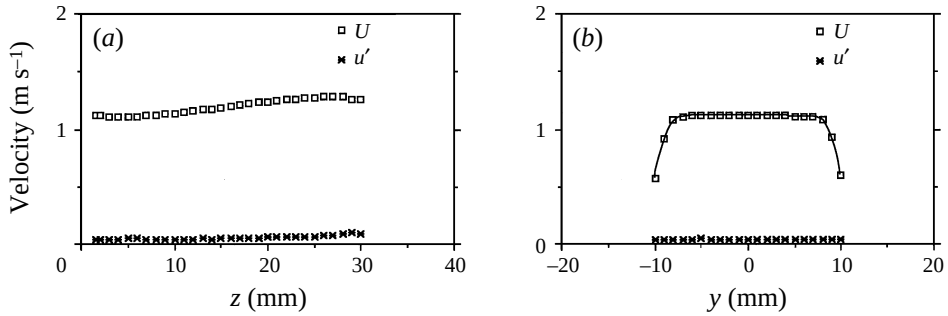

FIGURE 6. Flame without excitation. Equivalence ratio: 1.05. (*a*) Axial profiles of the mean and r.m.s. axial velocities, (*b*) radial profiles of the mean and r.m.s. axial velocities at $z = 1.5$ mm above the burner.

In the major part of the flame, the particle paths are straight and vertical, contrary to the case of 'V' flames on wires where the streamlines of the fresh gases are deflected outwards (De Sœte 1964; Escudié 1989). It is not possible to visualize deviations of the pathlines due to gas expansion in the flame preheat zone since the droplets disappear when the temperature reaches approximately 300 °C, i.e. close to the beginning of the thermal diffusion zone.

The axial profile of axial velocity in figure 6(*a*) shows, however, that there is a small increase in velocity, from 1.1 m s^{-1} at $z = 4$ mm to 1.25 m s^{-1} at the tip of the flame. The streamlines are slightly convergent due to the pressure gradient generated by the buoyant burnt gases. Figure 6(*a*) also shows a very slight drop in velocity between the burner exit and the plane $z = 4$ mm, related to the outwards deflection of the streamlines in the boundary layer, mentioned above. This has also been observed by previous authors (Wagner & Ferguson 1985; Baillot *et al.* 1992). Figure 6(*b*) shows that the radial profiles of the axial velocity at $z = 1.5$ mm are quite flat over the whole section.

3.2.2. *With acoustic excitation*

Figure 7 shows a tomographic cut of the hemispherical flame with an exposure time of 1/500 s corresponding to about 2 cycles of oscillation. The transition from a conical flame to an hemispherical flame will be examined later. The flame front appears slightly thickened, in a form of a flattened hemisphere. Droplet paths are clearly visible and show a strong deflection of the mean flow. The streamlines meet the

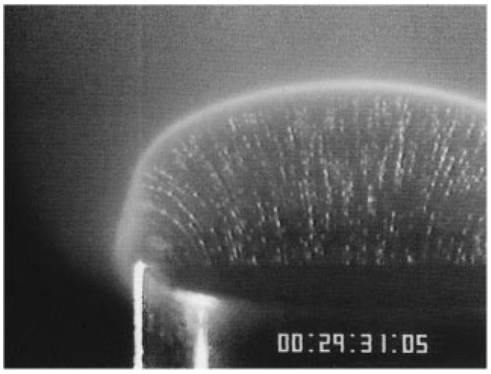

FIGURE 7. 'Hemispherical' flame. Equivalence ratio: 1.05. Space-averaged flow velocity: 0.92 m s^{-1}; r.m.s. velocity u' at the burner outlet: 1.25 m s^{-1}. Exposure time: 1/500 s.

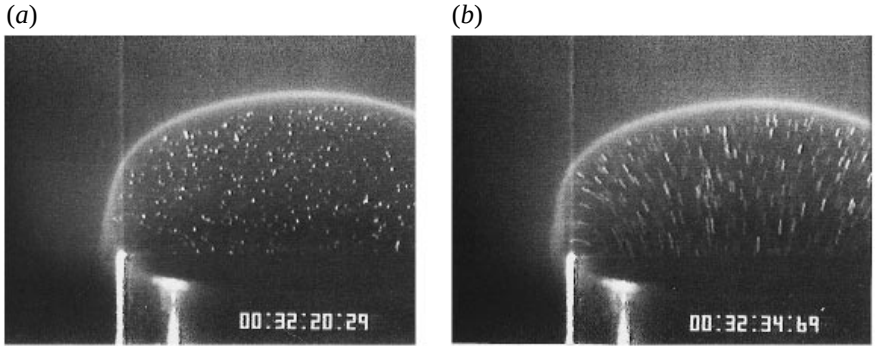

FIGURE 8. Two instantaneous photographs of the 'hemispherical' flame at times in phase opposition in the cycle. Exposure time 1/2000 s. In (*a*) the droplets are almost motionless. In (*b*) the trajectories show that the droplets have a high velocity.

flame front almost perpendicularly. Just above the edge of the burner, the luminous front is thicker and blurred.

Figure 8 shows two cuts taken with an exposure time of 1/2000 s, at times which are in phase opposition in the acoustic cycle. In figure 8(*a*) the particles have a minimal displacement; figure 8(*b*) shows particles in motion. Both photographs show that all droplets move in phase in the fresh gases. On the photograph with the larger displacement, path lengths at the burner exit are longer than those close to the flame front, showing that the intensity of the velocity oscillations decreases downstream.

Figure 9 shows axial profiles of the flow velocities. As anticipated, the mean and oscillating radial velocities on the axis are zero, figure 9(*b*). The mean axial velocity decreases regularly from 0.95 m s^{-1} at the burner exit down to 0.4 m s^{-1} at the position of the flame front ($z = 12$ mm), figure 9(*a*). This evolution is quite different from that observed in the cold jet, figure 3(*a*). This velocity decrease in the presence of the flame is linked to the strong deflection of streamlines. The mean velocity measured on the axis just ahead of the flame front is close to the laminar flame speed of the methane and air mixture. This result shows there is no modification of the physico-chemistry of the mixture under the action of the perturbation. This is to be be expected, since the acoustic time (10^{-3} s) is longer than the flame transit time (flame thickness/flame speed $\approx 10^{-4}$ s) which is the shortest time associated with the

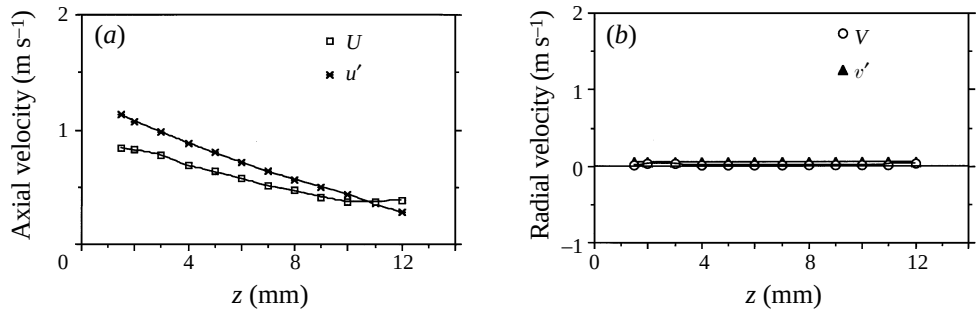

FIGURE 9. Streamwise profiles of velocities in the reacting flow. U and V are the mean axial and radial velocities, u' and v' are the corresponding r.m.s. components of the oscillation. Space-averaged flow velocity: 0.92 m s^{-1}. Frequency: 950.1 Hz.

combustion. The r.m.s. axial velocity decreases regularly with a slightly stronger slope than the mean velocity. At the burner exit, the velocity modulation is 1.25 m s^{-1}, which is less than the modulation in the cold jet, and it is about 0.35 m s^{-1} close to the flame front.

Figures 10(a) and 10(b) show the radial profiles of axial and radial velocities measured at five different heights from $z = 1.5$ mm up to $z = 9$ mm. The radial profile of the mean axial velocity at $z = 1.5$ mm, figure 10(a), is flat over the central region of the burner and has a slight increase just before the edge. As in the cold jet, the mean velocities are apparently negative just outside the edge of the burner. At $z = 3$ mm, the profile of the mean velocity becomes convex and this tendency increases as the flame is approached. The radial profiles of the r.m.s. velocity, u', are similar to those of the mean velocity. They are also similar to those measured in the cold flow, figure 4(a). At $z = 1.5$ mm, the profile is flat in the centre and shows a slight increase towards the edge. The profiles become convex with increasing altitude. They almost merge with those of U.

The radial profiles of the mean radial velocity V and the r.m.s. modulation, v', are shown figure 10(b). For all profiles the mean velocity has a regular radial gradient over a wide zone, between $y = -8$ mm and $+8$ mm. This gradient corresponds to the progressive deflection of the streamlines in the fresh gases. It should be remarked that at the outer edge of the flow ($y \approx \pm 10$ mm), the mean radial velocity is high but the mean axial velocity is close to zero, i.e. the mean flow has turned almost 90°.

The radial profile of the r.m.s. radial velocity, v', is similar to that of the mean radial flow, and also to the profile of v' in the cold flow. This v' value is obviously zero on the burner axis. At the periphery at $z = 1.5$ mm, v' reaches 1.5 m s^{-1}. This value is greater than the amplitude of u' measured on the axis at the same height. At the flame front and at $z = 1.5$ mm, the velocity modulation is therefore more than 3 times the laminar flame velocity. Further downstream, the radial gradient of v' is close to that of $|V|$. It decreases gradually with the height, but it remains strong, proving that the flow is deflected even near the top of the flame. The mean velocity of the flow on the edges at $z = 5$ mm, where the flame is very close to the vertical, can be calculated for the axial and the radial velocities, respectively equal to about 0.1 m s^{-1} and 0.35 m s^{-1}. It is close to the laminar adiabatic flame velocity.

In summary, the oscillating component of the flow is only slightly modified by the presence of the flame, whereas the mean flow is strongly modified and takes on a

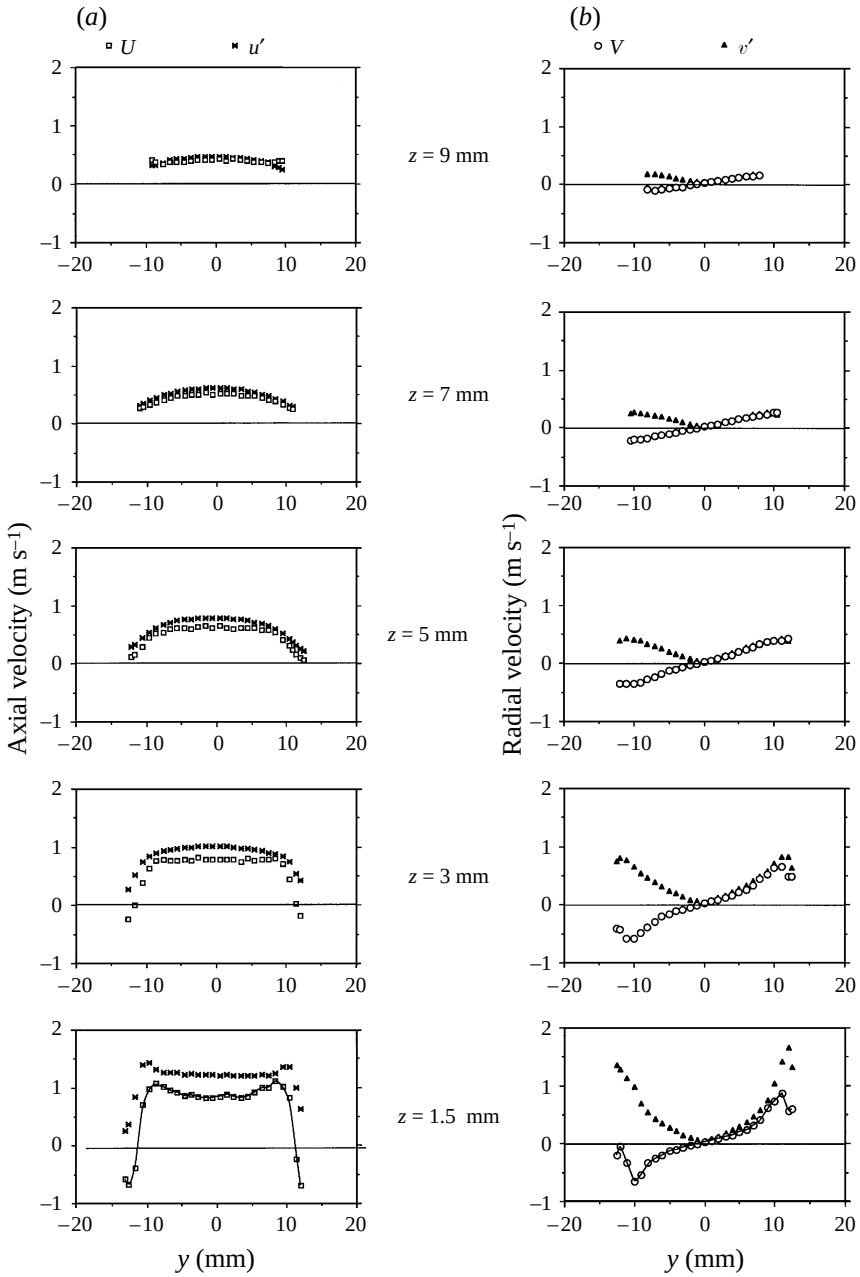

FIGURE 10. Radial profiles of velocities at different heights for the hemispherical flame. (*a*) Axial mean and r.m.s. velocities, (*b*) radial mean and r.m.s. velocities.

geometry which is close to that of the oscillating flow. Figure 11 (*a–d*) shows the velocity fields drawn from the above results.

A close observation of the films shows that the front is slightly displaced by the oscillating upstream flow. To confirm this statement, the oscillation frequency of the flame front has been measured near the edge of the burner where the displacement is maximal. The analogue signal of the photo-multiplier, used for LDV measurements,

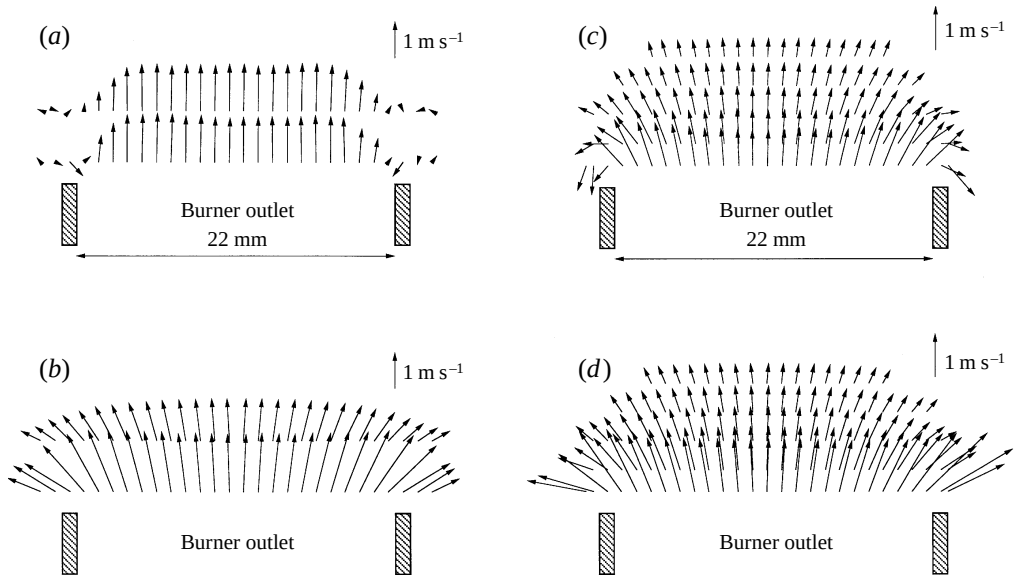

FIGURE 11. General view of the velocity fields: (*a*) and (*b*) mean velocity and r.m.s velocity respectively without flame, (*c*) and (*d*) the same fields with the presence of the flame

was sent directly to a spectrum analyser. The measurement volume was positioned on the isotherm where the seeding droplets evaporated. When the measurement volume was in fresh gases, droplets scattered the light and the signal was maximal; when the flame moved upstream, the measurement volume was in a non-seeded zone and the signal returned to zero. The total signal was therefore in the form of a square wave. The observed spectrum of this signal has a strong line centred on the acoustic frequency; thus the front is seen to oscillate at this frequency.

4. The surface area of the flame

An important point is the variation of the total surface area of the reaction zone when the flame becomes hemispherical under the action of the acoustic field. Four tests were carried out at frequencies of 800 Hz, 1000 Hz, 1800 Hz and 4000 Hz, in conditions where the flame had the form of a stable and flattened hemisphere. The amplitude of modulation was adjusted so that the height of the flame was the same in all cases. Between 2000 and 4000 Hz, it was not possible to obtain a hemispherical flame with this burner. This is probably due to the structure of the acoustic modes in the burner which limited the maximal velocity modulation for a fixed input power. The length of the downstream limit of the luminous region was measured using standard image processing and averaged over ten independent images. The flame area, S, was calculated supposing axial symmetry. The area of the unperturbed conical Bunsen flame, S_o, was also measured using the same technique. Figure 12 shows the ratio S/S_o obtained for the four excitation frequencies given above. The values range from 0.96 to 1.0; the maximum dispersion of the measurements for any flame was 5%. We thus conclude that there is no significant change in the surface area of the flame when it is deformed by an acoustic field of this amplitude. In other words, the laminar combustion velocity of the stoichiometric flame is unchanged. This conclusion is contrary to that of De Sœte (1964). Von Hahnemann & Ehret (1943) also reported a

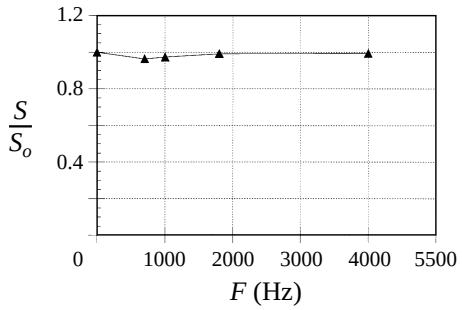

FIGURE 12. Surface area of the hemispherical flame for different frequencies. Equivalence ratio: 1.05. Space-averaged flow velocity: 0.92 m s^{-1}.

change in flame area; however their measurements were made on strioscopic images, corresponding to the position of the strongest thermal gradient. In their paper, no comparison was made between this position and the position of the reaction zone. This conservation of the flame surface area is not surprising because the characteristic chemical time of the reaction is smaller than the characteristic time of the forcing.

5. Transition from a conical to a hemispherical flame

The transition from the conical to the hemispherical flame is shown in figure 13. As the acoustic intensity is increased, the flame becomes cellular before becoming smooth and quasi-hemispherical. Six sets (*a* to *f*) of three photographs are shown. Each set corresponds to the same level of acoustic power. For all values cited in this paragraph, the r.m.s. acoustic velocity is measured on the axis at 1.5 mm above the exit plane of the burner. The photographs are presented in groups of three because a convective flow instability at a low frequency, about 15 Hz, perturbs the vertical Bunsen flame. This instability is due to the shear between the burnt gases and the ambient air (Durox, Yuan & Villermaux 1992). It creates regular vortices which are carried downstream and make the flame front oscillate. These vortices are sufficient to disturb the flame when it is close to conical. This explains the differences between the three photographs taken when the acoustic power is weak. The three photographs of each set are taken at times approximately equally spaced through a period of the low-frequency instability. In (*a*), the modulation depth u'/U_L is 1.16, but the flame is little deformed. However, a small deflection of the streamlines is visible close to the edge of the burner. In (*b*), small cells have formed around the flame tip and a weak undulation appears on the flame front. In the next stage (*c*), where u'/U_L equals 1.66, a large unstable horizontal cell, about 15 mm in diameter, has developed. The lateral edge of the flame front is almost rectilinear and the particle trajectories are distinctly inclined. The angle between the cell and the lateral edge of the flame front is sharp. On further increasing the acoustic power, several chaotic cells, about 8 mm in diameter, are formed perpendicular to the axis (photos *d*). In photos (*e*), some unstable cells remain on the top of the flame. In (*f*), u'/U_L equals 2.66 and the flame appears to be smooth and stable to the eye except for a blurred zone close to the burner edge where the velocity oscillations are strongest. When the particle trajectories are visible, they show a strong curvature. At this level of acoustic power the flame extends considerably beyond the burner radius.

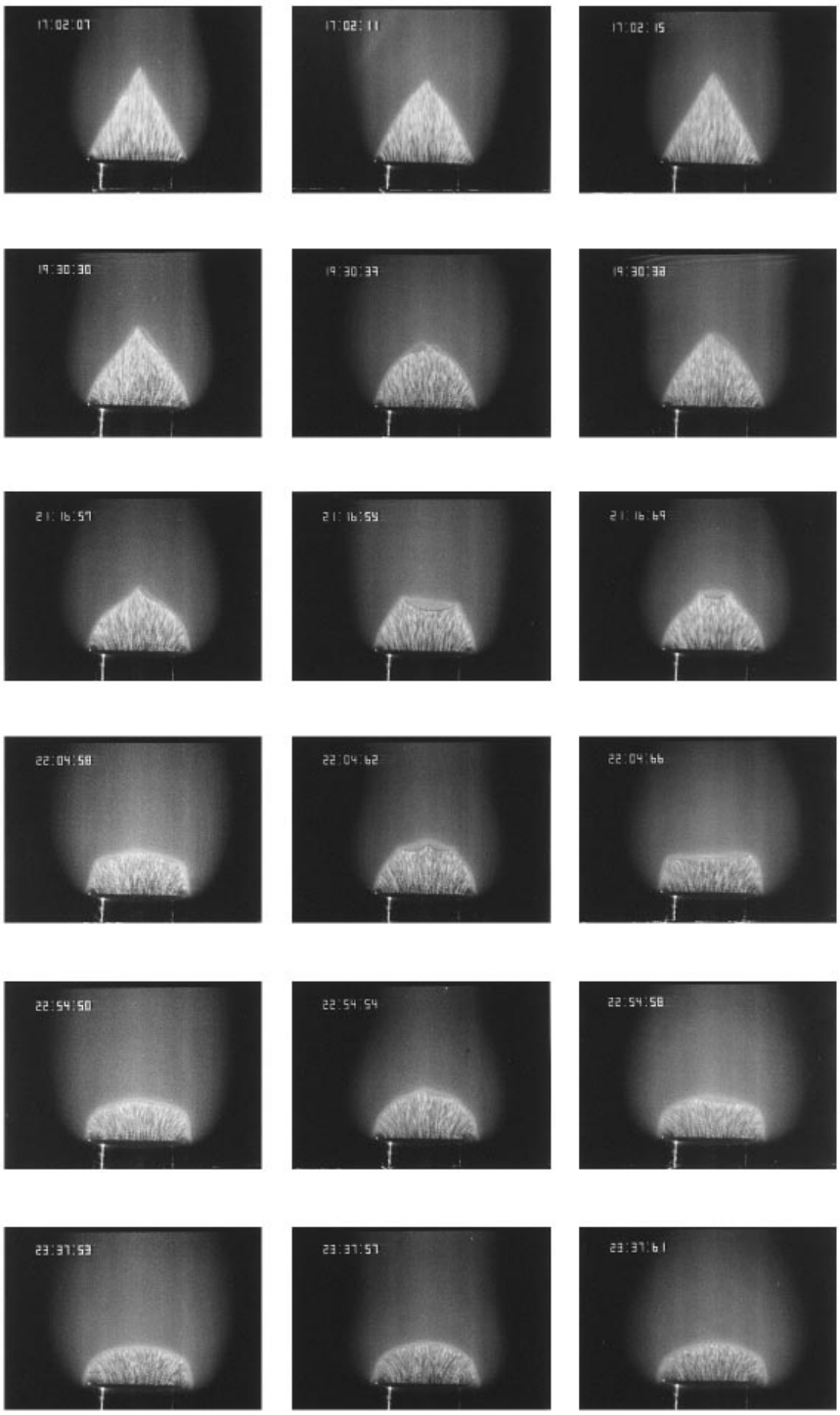

FIGURE 13. Transition between the laminar flame and the hemispherical flame. Exposure time:1/500 s. Flow rate: 0.92 m s^{-1}. Equivalence ratio: 1.05. Each set of photographs corresponds to the same level of acoustic power: (*a*) $u'/U_L = 1.16$, (*b*) $u'/U_L = 1.60$, (*c*) $u'/U_L = 1.66$, (*d*) $u'/U_L = 1.88$, (*e*) $u'/U_L = 2.30$, (*f*) $u'/U_L = 2.66$. For each set, three photographs are taken approximately equally spaced in phase during the low-frequency cycle of an outer flow instability. u' is measured on the axis at $z = 1.5$ mm above the burner.

6. Discussion

The transition to a smooth quasi-hemispherical flame under the influence of a strong acoustic field is analogous to the phenomenon of flame restabilization described by Searby (1992) for the case of a flame propagating in a tube. Searby has shown that in his configuration, the hydrodynamic Darrieus–Landau instability (Landau 1944) can be restabilized by an oscillating acoustic field when the ratio of r.m.s. acoustic velocity to laminar burning velocity exceeds a value of roughly 3 (Searby & Rochwerger 1991). In the present experiment, the conical flame front is deformed towards a quasi-hemispherical shape for a similar value of the acoustic velocity at the flame front. However, here the acoustic field is not confined, but radiated from the burner exit. We will argue below that the quasi-hemispherical shape of the flame is imposed by the geometry of the acoustic field radiated from the burner exit. The form of the mean flow field is then imposed by the modified mass flux boundary conditions at the new position of the flame front.

In the cold gas, the mean and the oscillating flow fields can be considered to be independent since the Mach number is small. If U_s is the norm of the mean velocity and U_a the acoustic amplitude, i.e. the norm of the oscillating part of velocity, the nonlinear coupling term in the Navier–Stokes equation, $(U_s/c)\omega U_a \equiv \mathrm{M}\omega U_a$, is small compared to the time-dependent term, ωU_a. For the same reason we can also neglect the existence of acoustic streaming whose amplitude is of order of U_a^2/c (Landau & Lifchitz 1989). We thus describe the total velocity field as a superposition of the mean field $\boldsymbol{U}_s(\boldsymbol{r})$ and an acoustic field $\boldsymbol{U}_a(\boldsymbol{r})$. Moreover, the near-field acoustic flow is close to potential flow over a distance small (here $\approx$ 20 mm) compared to the acoustic wavelength ($\approx$ 30 cm) since the amplitude of the acoustic displacement (here $\approx$ 1 mm) is small compared to the dimensions of the flow (here $\approx$ 20 mm) (Landau & Lifchitz 1989). The acoustic velocity field $\boldsymbol{U}_a = u_a\boldsymbol{x} + v_a\boldsymbol{y} + w_a\boldsymbol{z}$ (u' and v' are the r.m.s. values of u_a and v_a) can thus be written as the gradient of some potential function:

$$\boldsymbol{U}_a = \nabla\varphi\,(\boldsymbol{r}, t) = \nabla\varphi\,(\boldsymbol{r})\,\mathrm{e}^{\mathrm{i}\omega t}.$$

The local acceleration

$$\gamma_a = \mathrm{d}\boldsymbol{U}_a/\mathrm{d}t$$

in the above approximation is thus colinear with $\boldsymbol{U}_a$ and finally the local acceleration is perpendicular to the equipotential surfaces. It is observed experimentally that the presence of the flame has only a small effect on the acoustic field in the unburnt gas, see figures 4 and 10.

Searby & Rochwerger (1991) have shown that the presence of an acoustic field drives the front towards a surface perpendicular to the local acceleration. In the presence of a periodic (acoustic) acceleration, the dynamics of a freely propagating flame front are governed by a parametric oscillator equation in wavenumber space. For zero- or small-amplitude acoustic fields, there exists a large range of wavenumbers giving rise to solutions with time-increasing amplitudes, corresponding to the well-known Darrieus–Landau instability. For moderate acoustic fields (defined by $U_a \approx 5U_L$) which are however of order 140 dB, the solutions to the equation can have time-decreasing amplitudes at all wavenumbers. The stationary state is obtained when the flame front is perpendicular to the acoustic acceleration and parallel to an equipotential of the acoustic field.

A heuristic explanation of the restabilization is as follows: the equipotential surfaces of the acoustic fields are also surfaces of constant pressure. During the half-cycle of the acoustic period in which the acceleration is directed towards the burnt gas,

any difference in altitude with respect to an equipotential surface will create pressure gradients that tend to displace the fluid and decrease this difference. This is analogous to the effect of gravity on a water–air interface. During the other half of the acoustic period, the opposite effect occurs. However, when inertia of the fluid is taken into account, the situation is not symmetrical. For a limited range of acoustic accelerations, the net effect of each complete acoustic cycle can leave the flame front closer to the equipotential surface. This situation is completely analogous to that of an unstable pendulum restabilized by a vertically oscillating reference frame (Landau & Lifchitz 1982; Arnold 1980).

In the experiment of Searby & Rochwerger, the equipotential surfaces were planar. In the present experiment, the exact form of the potential function associated with a circular source is not known analytically, except at the burner exit where the equipotential surfaces of the flow are planar and in the far field where they tend rapidly towards a hemispherical form when the distance is greater than the burner diameter. For the same reason it is not possible to calculate the stability limits analytically in this axisymmetric geometry. However, from the reasoning presented above, we expect that the conical front of the Bunsen flame will be driven towards an equipotential surface of the radiated acoustic field when the amplitude of the acoustic velocity U_a at the flame front is of the order of $5U_L$. We may note that the acoustic acceleration ωU_a in our experiment is of the order of 10 000 m s^{-2} (1000 g) and the pressure exerted on a column of unburnt gas of height 2 cm subjected to this acceleration in a bath of burnt gas is about 200 Pa. This is very much greater than the stagnation point pressure, $\rho U^2 \approx 1$ Pa, of the mean flow at the burner exit, showing that pressure gradients created by the acoustic field may indeed greatly modify the mean flow.

The shape of the flame front is thus imposed by the acoustic field which drives the front towards an equipotential surface of the acoustic field. The flame will eventually position itself on the equipotential surface whose area is equal to the area of the conical flame. This, in turn, imposes a new boundary condition for the mean flow field. The total mass flux from the burner is fixed by the experiment. The normal mass flux at the flame front is fixed by the flame chemistry and is equal to the laminar flame velocity, U_L, times the gas density. The mean flow field in the presence of the curved flame must now adjust itself so that the normal mass flux at the flame front is everywhere equal to this fixed value. If we suppose, for instance, that to a first approximation the equipotential surfaces for the acoustic field are spherical, then the mean flow will be necessarily radial by symmetry. Von Hahnemann & Ehret (1943) have shown that the flame shape is indeed close to that of the experimentally measured shape of an equipotential surface in an electrostatic analogue of the burner. However these authors were not able to justify this observation. In a recent numerical simulation of the same flame configuration, Jenny (1997) also has observed the transition of a conical flame to a curved flame whose shape is close to an equipotential surface of the acoustic field.

In summary we observe a most peculiar effect: the oscillating flow has imposed its geometry on the mean flow. The acoustic forcing has imposed a specific shape and position for the density interface (flame front), separating the burnt and unburnt gas. The amplitude of the displacement of the front is very small (0.2 mm) compared to the dimensions of the burner and may be considered as a fixed surface with respect to the mean flow. The modified shape of the flame front, imposed by the forcing, associated with the necessary condition of mass flux through the front creates a new 'exotic' boundary condition to which the mean flow must adapt itself. This is quite

contrary to the normal case of a freely propagating flame in which the flow field is considered as being imposed and in which the flame front adapts its position and shape so that the component of the flow normal to the flame front is equal to the laminar flame velocity U_L. In the case of the conical flame without forcing, the angle between the flame front and the flow decreases as the gas speed increases.

We compare the theoretical results concerning the stability domain given by Searby & Rochwerger (1991) for a planar flame with the observations of the present experiment. Here, the restabilization is obtained for an r.m.s. acoustic velocity which is not strictly constant along the flame front and which is in the range $2U_L$ to $3U_L$, whereas Searby & Rochwerger calculate that the restabilization threshold occurs for a ratio $u'/U_L \approx 3.5$. Taking into account the substantial differences in the geometry between the two experiments we consider that this result is in reasonably good agreement with our observations.

7. Conclusion

Strong acoustic forcing at high frequency (of the order of 1000 Hz) leads to a strong deformation of a conical flame which deforms to a flattened hemisphere above the burner exit.

The velocity modulation required to reach this state is of the order of $u'/U_L = 3$ at the exit of the burner for a stoichiometric methane–air flame subjected to frequencies of the order of 1000 Hz. The disappearance of the cellular structures and the smoothing of the flame are reminiscent of the primary parametric restabilization observed for flames propagating in tubes. However, in the present experiment, the configuration is quite different: the flame is outside the tube, and it adapts its shape to follow one of the equipotential surfaces of the acoustic field. The new boundary condition imposed by this new flame shape then forces the mean flow to diverge until the mean flow velocity normal to the flame front is everywhere equal to the laminar flame velocity. In other words the geometry of the oscillating acoustic flow controls the geometry of the stationary flow.

The study of the flame surface area contradicts the previous results of De Sœte (1964) and of von Hahnemann & Ehret (1943), who reported a decrease of the measured flame area. Our measurements show that, at unit equivalence ratio, when the flame is flattened, the flame surface area remains unchanged, i.e. the reaction rate is unaffected by the acoustic perturbation.

The use of a higher acoustic intensity and a smaller laminar flame velocity should allow observation of the secondary parametric instability already observed on flames propagating in tubes. This work is in progress.

This study was supported by DRET under contract N 90.34.193.

REFERENCES

Arnold, V. I. 1980. *Mathematical Methods of Classical Mechanics*, p. 121. Springer.

Baillot, F., Durox, D. & Prud'homme, R. 1992 Experimental and theoretical study of a premixed vibrating flame. *Combust. Flame* **88**, 149–168.

Bourehla, A. 1994 Instabilités forcées d'une flamme vibrante conique de prémélange. PhD thesis, Université Pierre et Marie Curie, Paris VI.

Boyer, L. 1980 Laser tomographic method for flame front movement studies. *Combust. Flame* **39**, 321–323.

Bruneau, M. 1983 *Introduction aux Théories de l'Acoustique*. Université du Maine Editeur.

Clanet, C. & Searby, G. 1994 Acoustic instability in one-phase and two-phase combustion. In *Euromech 324, 'The Combustion of Drops, Sprays and Aerosols, Marseille.*

Clavin, P., Pelcé, P. & He, L. 1990 One-dimensional vibratory instability of planar flames propagating in tubes. *J. Fluid Mech.* **216**, 299–322.

De Sœte, G. 1964 Étude des flammes vibrantes. Application à la combustion turbulente. *Revue de l'Institut Français du Pétrole et Annales des combustibles liquides*, vol. XIX(6).

Dunlap, R. A. 1950 Resonance of flames in a parallel-walled combustion chamber. *Aeronautical Research Center. University of Michigan, Project MX833, Rep.* UMM43.

Durox, D. & Baillot, F. 1993. About a bias of measurement found in a high frequencies pulsated reactin flow. In *5th Intl Conf. on Laser Anemometry – Advances and Applications, Veldhoven, Netherlands, 23–27 August.*

Durox, D., Schulz, B. & Rudent, P. 1995 Sensitivity of premixed flames submitted to sinusoidal excitation. In *Joint Meeting of the French and German Sections of the Combustion Institute, Mulhouse, France, 11–13 October.*

Durox, D., Yuan, T. & Villermaux, E. 1992 Influence of gravity and ambient pressure variations on behaviour of buoyant laminar diffusion flames. In *VIIIth European Symp. on Materials and Fluid Sciences in Microgravity, Brussels, 12–16 Avril*, ESA SP-333, vol. 2.

Escudié, D. 1989 Interaction of a flame front with vortices: an experiment. *Lectures Notes Engineering* (ed. R. Borghi & S. W. B. Murthy), vol. 40, p. 323. Springer.

Hahnemann, H. von & Ehret, L. 1943 Über den Einflußstarker Schallwellen auf eine stationär brennende Gasflamme. *Z. Tech. Phys.* **24**, 228–242.

Ingard, U. & Ising, H. 1967 Acoustic nonlinearity of an orifice. *J. Acoust. Soc. Am.* **42**, 6–17.

Jenny, P. 1997 On the numerical solution of the compressible Navier–Stokes equations for reacting and non-reacting gas mixtures. PhD thesis, ETH No.12030, Swiss Federal Institute of Technology, Zurich.

Kaskan, W. E. 1953 An investigation of vibrating flames. In *Fourth Intl Symp. on Combustion*, pp. 575–591. Williams and Wilkins.

Landau, L. 1944 On the theory of slow combustion. *Acta Physicochimica URSS*, 77–85.

Landau, L. D. & Lifchitz, E. M. 1982 *Mécanique*, 4th Edn, p. 149. MIR, Moscow.

Landau, L. D. & Lifchitz, E. M. 1989 *Mécanique des Fluides*, 2nd Edn, pp. 400, 437. MIR, Moscow.

Le Helley, P. 1994 Étude théorique et expérimentale des instabilités de combustion et de leur contrôle dans un brûleur laminaire prémélangé. PhD thesis, Ecole Centrale de Paris.

Leyer, J. C. & Manson, N. 1971 Development of vibratory flame propagation in short closed tubes and vessels. In *Thirteenth Symp.* (*Intl*) *on Combustion*, pp. 551–557. The Combustion Institute.

Markstein, G. H. 1953 Instability phenomena in combustion waves. In *Fourth Intl Symposium on Combustion*, pp. 44–59. Williams and Wilkins.

Markstein, G. H. 1964 *Nonsteady Flame Propagation.* Pergamon Press.

Pelcé, P. & Rochwerger, D. 1992 Vibratory instability of cellular flames propagating in tubes. *J. Fluid Mech.* **239**, 293–307.

Poinsot, T., Trouvé, A., Veynante, D., Candel, S. & Esposito, E. 1987 Vortex driven acoustically coupled combustion instabilities. *J. Fluid Mech.* **177**, 265–292.

Searby, G. 1992 Acoustic instability in premixed flames. *Combust. Sci. Technol.* **81**, 221–231.

Searby, G. & Rochwerger, D. 1991 A parametric acoustic instability in premixed flames. *J. Fluid Mech.* **231**, 529–543.

Wagner, T. C. & Ferguson, C. R. 1985 Bunsen flame hydrodynamics. *Combust. Flame* **59**, 267–272.